RSC Advances

PAPER

View Article Online
View Journal | View Issue

Cite this: *RSC Adv.*, 2021, **11**, 16510

The biofunctionalization of titanium nanotube with chitosan/genipin heparin hydrogel and the controlled release of IL-4 for anti-coagulation and anti-thrombus through accelerating endothelialization

Wen Peng Yu, †[a] Yi Gong,†[a] Ziyao Wang,[c] Chao Lu,[a] Jing Li Ding,[b] Xin Liang Liu,[a] Guo Dong Zhu,[a] Feng Lin,[a] Jian Jun Xu[a] and Jian Liang Zhou *[a]

The valve replacement is the main treatment of heart valve disease. However, thrombus formation following valve replacement has always been a major clinical drawback. Accelerating the endothelialization of cardiac valve prosthesis is the main approach to reduce thrombus. In the current study, a titanium nanotube was biofunctionalized with a chitosan/genipin heparin hydrogel and the controlled release of interleukin-4 (IL-4), and its regulation of macrophages was investigated to see if it could influence endothelial cells to eventually accelerate endothelialization. TNT60 (titanium dioxide nanotubes, 60 V) with nanoarray was obtained by anodic oxidation of 60 V, and IL-4 was loaded into the nanotube by vacuum drying. The hydrogel (chitosan : genipin = 4 : 1) was applied to the surface of the nanotubes following drying, and the heparin drops were placed on the hydrogel surface with chitosan as the polycation and heparin as the polyanion. A TNT/IL-4/G (G = gel, chitosan/genipin heparin) delivery system was prepared. Our results demonstrated that the biofunctionalization of titanium nanotube with chitosan/genipin heparin hydrogel and the controlled release of IL-4 had a significant regulatory effect on macrophage M2 polarization, reducing the inflammatory factor release and higher secretion of VEGF (vascular endothelial growth factor), which can accelerate the endothelialization of the implant.

Received 1st November 2020
Accepted 18th April 2021

DOI: 10.1039/d0ra09295a

rsc.li/rsc-advances

Introduction

The valve replacement is the main treatment of heart valve disease. However, several disadvantages have been encountered with regard to the application of prosthetic valves in clinical treatment. Among them, thrombus formation following valve replacement has always been a major clinical drawback. Recent studies have shown that rapid endothelialization of implant materials can effectively reduce platelet adhesion, reduce the receptor immune response and the risk of thrombosis due to endothelial cell coverage.[1]

Titanium (Ti) is widely used in all types of blood contact materials and devices, such as thrombus filters and artificial heart valves. However, it is still necessary to improve its medical application performance, while maintaining its other beneficial properties.[2] Titanium dioxide nanotubes have a wide range of potential applications due to their nano properties, low toxicity, good biocompatibility, inherent characteristics and multifunctional manufacturing technology.[3,4] Therefore, the conversion of titanium into titanium dioxide by surface modification has become a research hotspot of implant materials.[3,4]

When the material is implanted into the host, the host's response to the material begins immediately, including protein adhesion, cellular response, acute inflammation, chronic inflammation, granulation tissue formation and eventual formation of the package, which are successive and overlapping stages.[5,6] Macrophages mediate the initial immune response and play an irreplaceable role. The phenotype of macrophages includes two representative phenotypes, namely pro-inflammatory M1 and anti-inflammatory M2. Macrophages are induced into pro-inflammatory M1 or anti-inflammatory M2 phenotypes under different microenvironments. IFN and LPS can promote macrophage M1 polarization, and subsequently cause the secretion of TNF-α (tumor necrosis factor-α), IL-1 (interleukin 1), IL-6 (interleukin 6), iNOS (inducible nitric

[a]*Department of Cardiovascular Surgery, The Second Affiliated Hospital of Nanchang University, No. 1 Minde Road, Nanchang 330006, Jiangxi, China. E-mail: zhoujianliang2010@163.com; Tel: +86 137 6711 7511*

[b]*Department of Gastroenterology, The Second Affiliated Hospital of Nanchang University, Nanchang, China*

[c]*Department of Clinical Pathology, The First Affiliated Hospital of Gannan Medical College, Ganzhou, China*

† These authors contributed equally: Wenpeng Yu and Yi Gong.

oxide synthase) and similar cytokines. In contrast to these findings, IL-4 can promote macrophage M2 polarization and stimulate the secretion of cytokines that reduce inflammation and facilitate tissue repair, such as IL-10 (interleukin 10), ARG1 (arginase-1) and VEGF (vascular endothelial growth factor).[7] Therefore, regulating the polarization of macrophages can effectively control the occurrence of inflammation and the repair of the tissues.[8]

A series of physiological activities of endothelial cells (proliferation, adhesion and migration) play an indispensable role in preventing blood coagulation and thrombosis.[9] Endothelial cells line the vascular lumen and regulate the dynamic pathways of nutrients and cells. Furthermore, angiogenic growth of the vascular system is an example of the close coordination of cell proliferation, differentiation, migration, matrix adhesion, and cell–cell signaling processes.[10]

Based on the drug loading function of the TNT and good medical biological properties, we designed the TNT drug delivery system. Heparin with an anticoagulant effect was initially released. Subsequently, IL-4 cytokines that promoted M2 polarization were released, with the ultimate goal of accelerating endothelialization and reducing thrombosis. In this drug delivery system, a hydrogel system was added. Hydrogels have been widely used in drug delivery systems with optimal biocompatibility and biodegradability of natural polymers. Chitosan is a polysaccharide with optimal biodegradability, biocompatibility, film-formation ability and reduced toxicity.

Materials and methods

Materials

NH_4F (Macklin, China). Polyethylene glycol (Sinopharm, China). Mouse IL-4 protein (R&D, USA). Heparin (Sangon Biotech, China). Carboxymethyl chitosan and Genipin (Aladdin, China). Matrigel (BD Biosciences, USA). IL-4 Kit, IL-1 Kit, IL-6 Kit, IL-10 Kit and TNF-α Kit were purchased from R&D (USA). Heparin sodium test Kit (Leagene Biotechnology, China).

Animal

Six-week old female C57 mice were selected for the experiment. Mice were maintained in a specific pathogen-free facility. The New Zealand rabbit was obtained from the Nanchang University Animal Experiment Center for blood collection. All animal experiments were approved by the Animal Experimental Ethics Association of the Nanchang University.

Cell culture

Mouse macrophages (Raw264.7) and mouse endothelial cells (C166) were purchased from ATCC. The cells were cultured using α-MEM medium containing 10% FBS at 37 °C and in the presence of 5% CO_2. RAW cells were planted on the surface of the materials that were treated under different conditions, and the cell supernatant was collected. The same amount of α-MEM medium was added to form a conditioned medium (CM).

Preparation of the TNT/IL-4/G delivery system

Preparation of TNT60. Titanium was polished with strong acid ($HF : HNO_3 : H_2O = 1 : 4 : 5$) for 60 s. TNT was prepared by anodization. The electrolyte used was NH_4F (2.6 g), polyethylene glycol (450 mL), and double distilled water (50 mL). A 60 V electrolysis was run for 1 h. Ultrasonic cleaning of anhydrous alcohol following electrolysis was performed for 3 min. Subsequently, ultrasonic cleaning was performed twice by double distilled water. Finally, TNT60 was obtained. The obtained TNT60 was sterilized under ultraviolet light for 1 hour, and preserved for further study.

IL-4 and heparin loading on TNT. A total of 20 μL of mouse IL-4 protein (50 ng μL^{-1}) was placed on the surface of TNT with a diameter of 35 mm. The IL-4 was loaded into the TNT by vacuum drying. A layer of hydrogel was applied to the TNT that had been loaded with IL-4. The hydrogel consisted of carboxymethyl chitosan (10 mg mL^{-1}) and genipin (5.65 mg mL^{-1}). TNT covered with hydrogel was labeled as TNT/H (no load of IL-4 and heparin). Subsequently, heparin was dissolved to 35 ng μL^{-1}. A total of 20 μL heparin was placed on the surface of the hydrogel at 37 °C. Chitosan was selected as the polycation and heparin as the polyanion. The two molecules were integrated. The final sample was denoted as TNT/IL-4/G. The Ti discs was sterilized under UV light for 1 hour before the assay. The schematic diagram of the preparation process is shown in Fig. 1.

Cytotoxicity assay. Macrophages were seeded in 96-well plates at a density of 10^4 cells per well. After incubation for 24 hours, the cells were treated with different nanocomposites for 24 hours. Relative cytotoxicity was assessed by MTT analysis.

Material characterization and release profiles. The surface topography and morphology of the samples were characterized by scanning electron microscopy (SEM, JEOL JSM-6700F, Japan). IL-4 and heparin release from TNT/IL-4/G were measured indirectly. TNT/IL-4/G was soaked in 1 mL PBS for 12 h, 1, 2, 3, 5, 7 and 11 days, and shaken at 37 °C. IL-4 was detected by ELISA kit. Heparin was measured according to the heparin sodium test kit instructions.

Polarization of macrophages on materials

Expression of polarization-related genes. The mRNA expression was detected by RT-PCR. We have divided them into five groups: Control, Ti, TNT, TNT/H, TNT/IL-4/G. Before the experiment, it should be disinfected under UV lamp. Samples from each group were co-cultured with macrophages, and only macrophages were found in the Control group. Total RNA was extracted when the confluence of cells reached about 85%. The total RNA was extracted by the RNeasy Mini kit (QIAGEN, Germany). Reverse transcription was subsequently carried out using the PrimeScript 1st Strand cDNA Synthesis kit (TaKaRa, Japan). Finally, gene amplification was detected using the Bio-Rad Quantitative Real-time PCR System (Hercules, CA, USA). Four M1 polarization-related genes (IL-1, IL-6, iNOS, TNF-α) and two M2 polarization-related genes (ARG1, CD206) were detected. The expression levels were standardized according to the levels of the GAPDH housekeeping genes, and the specific

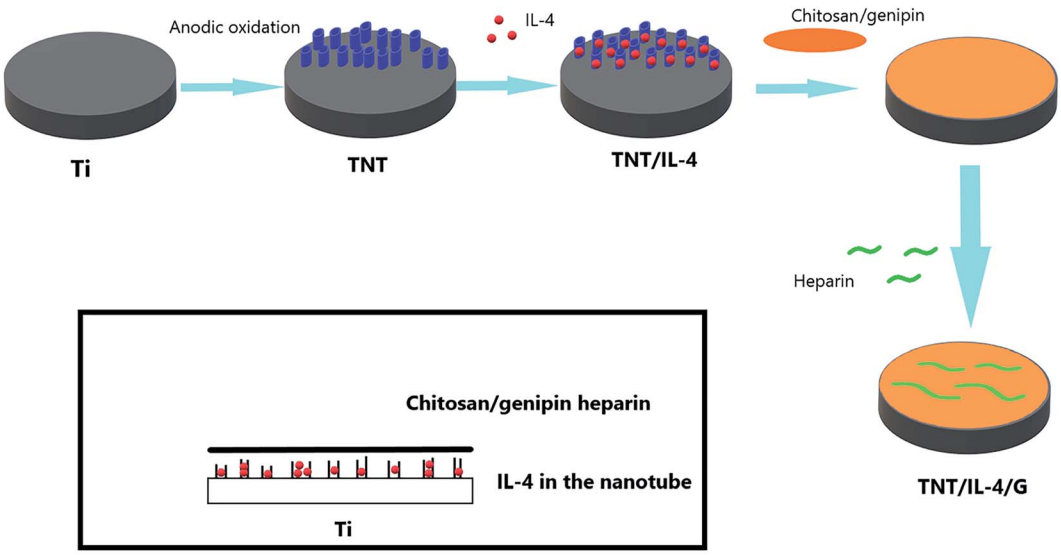

Fig. 1 Schematic diagram of the preparation process of TNT/IL-4/G.

Table 1 Primers used in this study[a]

Gene and primer direction		Sequence (5′ to 3′)
Mouse GAPDbH	Forward	AAGAAGGTGGTGAAGCAGG
	Reverse	GAAGGTGGAAGAGTGGGAGT
Mouse ARG	Forward	AGGAGATGCAAAGGAGGAA
	Reverse	CCTACCACACCAAAAGCC
Mouse CD206	Forward	TGGCAAGTATCCACAGCA
	Reverse	GGTTCCATCACTCCACTCA
Mouse IL-10	Forward	GCCCTTTGCTATGGTGTC
	Reverse	TCTCCCTGGTTTCTCTTCC
Mouse IL-1	Forward	AAGGAGAACCAAGCAACGACAAAA
	Reverse	TGGGGAACTCTGCAGACTCAAACT
Mouse IL-6	Forward	AGCCCACCAAGAACGATAG
	Reverse	GGTTGTCACCAGCATCAGT
Mouse iNOS	Forward	ACTCAGCCAAGCCCTCA
	Reverse	CTCTGCCTATCCGTCTCGT

[a] Abbreviations: GAPDH, glyceraldehyde-3-phosphate dehydrogenase; ARG, arginase; CD206, mannose receptor; IL, interleukin; iNOS, inducible nitric oxide synthase.

primer sequences are shown in Table 1 (Sangon Biotech, China).

Inflammatory factor detection. The macrophage supernatant was collected, and the expression levels of IL-1, IL-6, IL-10 and TNF-α were detected by ELISA kit (R&D, USA). The plate was initially immersed in blocking buffer. Subsequently, the standard and sample were mixed with the specific primary antibody (1 : 100 dilution) and incubated at room temperature for 1.5 h. Following washing for 6 times with PBST, the secondary anti-horseradish peroxidase (HRP) was added for 30 min. The coloring and stop solutions were added in sequence, and the absorbance was monitored with a 450 nm filter.

Effects of conditioned medium (CM) on C166 cells. The scratch test was used to analyze the migratory ability of the endothelial cells. C166 cells were seeded in 6-well plates. CM and ordinary medium were mixed in 1 : 1 into the wells. The cell growth traces were observed following 6 h and photographed. Image-J software was used for scratch area analysis.

To assess the proliferation of HUVECs in different conditioned media, 2×10^4 cells were seeded in 96-well plates. After 1, 3, or 5 days, 10 μL CCK8 solution was added to each well. The cells were incubated for 2 hours, and then the absorbance at 450 nm was measured with a microplate reader.

The Matrigel is often used as an *in vitro* angiogenesis model. A total of 50 μL Matrigel was added to a 96-well plate, and placed in an incubator at 37 °C for 30 min to solidify. A total of 4×10^5 cells per mL were placed on the Matrigel and photographed, following 6 h of culture in CM. Image-J was used for analysis of the total tube length and the number of branch points per field.

The determination of the anticoagulation efficiency *in vitro*

Blood coagulation time (BCT). Blood samples from New Zealand rabbits were collected in centrifuge tubes containing 3.8% sodium citrate. The samples were placed into a 24-well plate containing 0.5 mL phosphate buffer saline (PBS, pH = 7.4) per well, and collected from each group in 1.5 mL centrifuge tubes following 12 h of incubation. The control group contained equal doses of PBS. The samples were added to 5 mL glass tubes, and incubated at 37 °C for 5 min. Subsequently, 1 mL of rabbit blood containing sodium citrate was mixed and incubated at 37 °C for 3 min. A total of 500 μL calcium chloride solution (0.025 mol L^{-1}) was added to the tube to trigger coagulation. The tube was removed from the water bath and inverted every 15 s until the blood in the tube stopped flowing (inversion degree of up to 180°). The coagulation time was recorded as BCT.

Activated partial thromboplastin time (aPTT) and prothrombin time (PT). Blood samples from New Zealand rabbits were collected and diluted in test tubes containing 3.8%

sodium citrate at a ratio of 9 : 1. The samples were placed into a 24-well plate containing 0.5 mL PBS in each well. The PBS was removed following 12 h of incubation. A total of 1 mL blood was added to the centrifuge tube and vortexed. PT and aPTT were detected and recorded by the qLabsR Veterinary coagulation detector QV-1 (Micropoint Corporation, China).

Platelet adhesion. The blood samples were collected in the same way. Platelet-rich plasma (PRP) was obtained from these samples by secondary centrifugation (215 g and 863 g centrifugation, respectively, for 10 min). The samples were transferred into the 24-well plate, and 0.5 mL PRP was added to the plate that was covered and incubated at 37 °C for 12 h. Unattached platelets were removed by rinsing 5 times with PBS. Following washing with PBS, 0.25 mL of 1% Triton X-100 (diluted with PBS) was added to dissolve the attached platelets at 37 °C for 1 h. The lysates were analyzed using the LDH/LD kit (AMEKO, China), and the adherent platelet concentration was calculated based on the calibration curve. The calibration curve was determined by spectrophotometry as follows: the optical density of a range of known concentrations of platelets was measured at 450 nm.

***In vivo* animal studies.** The animals were anesthetized by intraperitoneal injection of 100 mg kg^{-1} sodium pentobarbital. Following sterilization with alcohol, a scalpel was used to cause a small opening in the back of the mouse. Subsequently, the scissors were used to bluntly separate the subcutaneous tissue until the material could be placed. The material was placed and the incision was sutured. Following 2 weeks of feeding, the material was removed and the angiogenic structure on the surface of the material was observed and photographed. The schematic diagram of the experimental steps is shown in Fig. 8E. The tissue was attached to the surface of the material, and was stripped of 4% paraformaldehyde overnight. The sections were further embedded and H&E staining was performed to observe the general structure of the sample. Immunohistochemical staining was used to detect CD31 expression (Abcam, Cambridge, UK). The images were obtained with a fluorescence microscope, and the fluorescence intensity was analyzed by the Image-J software.

Statistical analysis. The data are presented as mean ± SEM. All trial data were from at least 3 independent replicates. Statistical analysis was performed using the GraphPad Prism 7, and the one-way ANOVA test was used for determination of significant differences. A P value lower than 0.05 ($P < 0.05$) was considered for significant differences.

Results and discussion

Characterization of the titanium dioxide nanotube

Electron microscopy was performed on the nanotubes treated with different treatments (Fig. 2). Initially, the surface was explored with regard to the characteristics of pure titanium (Fig. 2A). The pipe diameter and length of TNT60 prepared by 60 V voltage were 110.80 ± 6.80 nm and 1698.71 ± 107.78 nm, respectively (Fig. 2B, C and F). The characterization of the TNT/IL-4/G drug delivery system is shown in Fig. 2D. We can observe that TNT was covered by a hydrogel. The thickness of the hydrogel layer was approximately 1515.43 ± 264.08 nm (Fig. 2E and F).

According to the anodizing mechanism, the tubular structure is produced by corrosion from the surface to the inside. During the anodizing process, if a larger anodizing voltage is applied, more F^- ions may accumulate on the surface, resulting in more severe corrosion and larger diameter nanotubes.[11] At the same time, the corrosion rate increases with the increase of voltage, so the length of the nanotubes increases with the increase of voltage when the same oxidation time is applied.

In vitro release of heparin and IL-4

The stable and sustained release of heparin and IL-4 was the main endpoint examined in the present study. PBS was collected from the orifice plates at various time points, and the release of heparin and IL-4 was measured using ELISA according to the instructions of the corresponding kit. As shown in Fig. 3, the release rate of the two release curves was gradually decreased with the extension of the culture time period. However, the rate of release of both is relatively gentle. The final cumulative release rate reached 82.8% ± 2.8% (heparin) and 72.5% ± 4.0% (IL-4), respectively. As shown in Fig. 3B, TNT, TNT/H, and TNT/IL-4/G all showed high cell activity, especially TNT/IL-4/G.

As an excellent natural biological crosslinking agent, genipin can be cross-linked with chitosan to make biological materials, such as artificial bones, wound dressing materials, and other materials, whose toxicity is far lower than glutaraldehyde and other commonly used chemical crosslinking agents. Chitosan also has good biocompatibility, biodegradability and the ability to accelerate wound healing, and is considered as an environmentally friendly material.[12] The data showed that IL-4 and heparin were released steadily without interference. Although the hydrogel layer is thin, which results in the simultaneous release of IL-4 and heparin, the main role of the gel layer is retained.[13] We used this positively charged material to assemble the chitosan/heparin-hydrogel with heparin. In the initial stage, the release of drugs in the hydrogel was mainly due to the swelling effect of the hydrogel. At the later stages of the release, it was due to the degradation of the chitosan/heparin-hydrogel.[14,15]

Macrophage polarization

Following confirmation of the stable and sustained release of heparin and IL-4, we performed RT-PCR analysis to assess the gene expression levels of these biomarkers in M1 and M2 macrophages that were present in different materials. We tested a total of five groups of samples, namely Control, Ti, TNT, TNT/H and TNT/IL-4/G. It can be intuitively noted that on days 1 or 3, the M2-related genes, with the exception of the relatively decreased expression of CD206, were upregulated to similar levels as those for ARG and IL-10. However, M2-related genes were upregulated on days 5 or 7 and the TNT/IL-4/G delivery system exhibited the highest expression of these genes, followed by TNT and TNT/H. A significant difference was noted between the TNT/IL-4/G and the control group ($P < 0.01$)

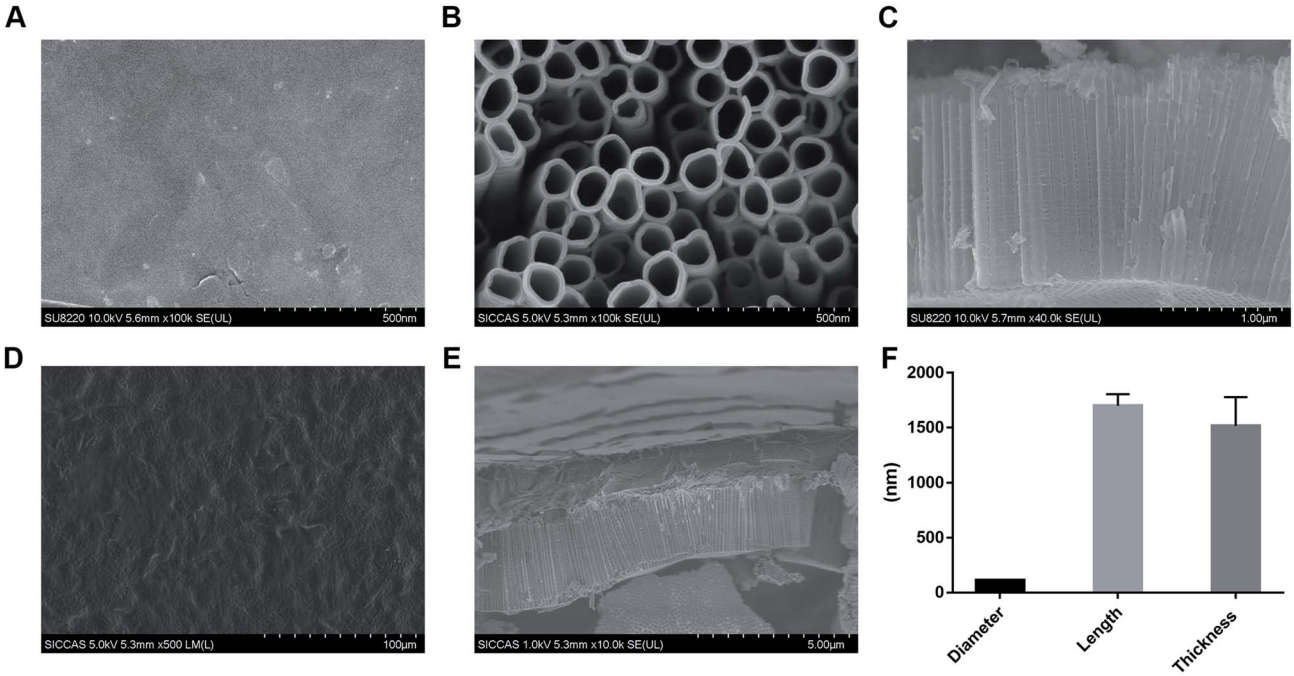

Fig. 2 Characterization of nanotubular surfaces. (A) The surface morphologies of Ti observed using SEM. (B) The surface morphology of TNT was observed by SEM. (C) SEM shows the length of TNT. (D) TNT/IL-4/G drug delivery system was characterized by SEM. (E) The thickness of hydrogels was scanned by SEM. (F) The length of titanium dioxide nanotubes and the thickness of the hydrogel. Results are presented as mean, $*P < 0.05$, $**P < 0.01$.

(Fig. 4A–C). The expression levels of the M1-related genes, such as IL-1, IL-6 and iNOS, were increased with the exception of Ti, which exhibited decreased expression in the macrophages of other nanotubes, notably in the TNT/IL-4/G group ($P < 0.05$) (Fig. 4D–F).

Previous studies in multiple tissues and organ systems have shown that in the early stages of the post-implantation inflammatory response, the materials that cause improved tissue repair or organ remodeling are often associated with the conversion of M1 macrophages to M2 macrophages.[16] Analysis of the abovementioned test results shows that the biological properties exhibited by TNT/IL-4/G have indeed transformed macrophages into M2 type, which is the same as our point of view.

Detection of the expression of inflammatory cytokines

The supernatant samples of the Ti, TNT60, TNT/H and TNT/IL-4/G were extracted to detect the concentration levels of the inflammatory cytokines secreted by the macrophages. IL-1, IL-6 and TNF-α were the three main inflammatory cytokines that were secreted by the M1-type macrophages. As shown in Fig. 5A, B and D the expression levels of the inflammatory factors in the

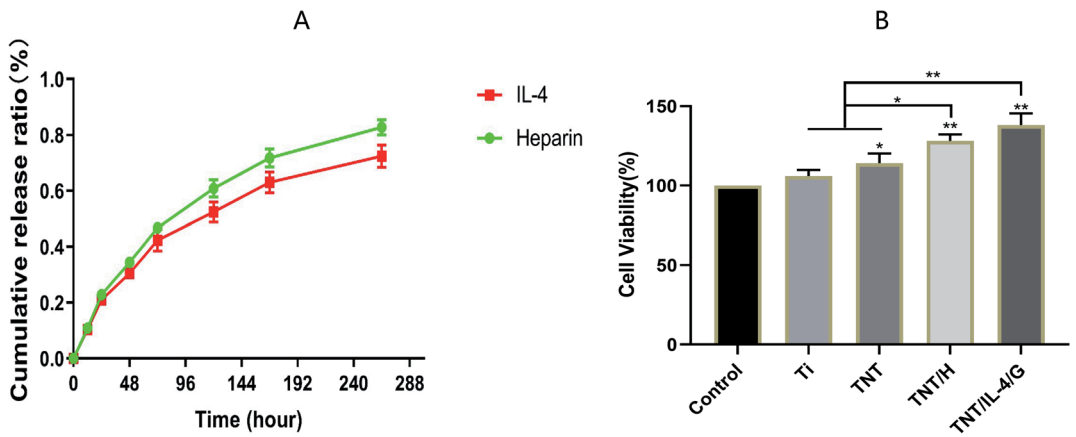

Fig. 3 (A) *In vitro* release of heparin and IL-4. IL-4 and heparin release were detected in TNT/IL-4/G delivery systems at 12 h, 1 d, 2 d, 3 d, 5 d, 7 d and 11 d. (B) Cytotoxicity was detected in each group. Results are presented as mean, $*P < 0.05$, $**P < 0.01$.

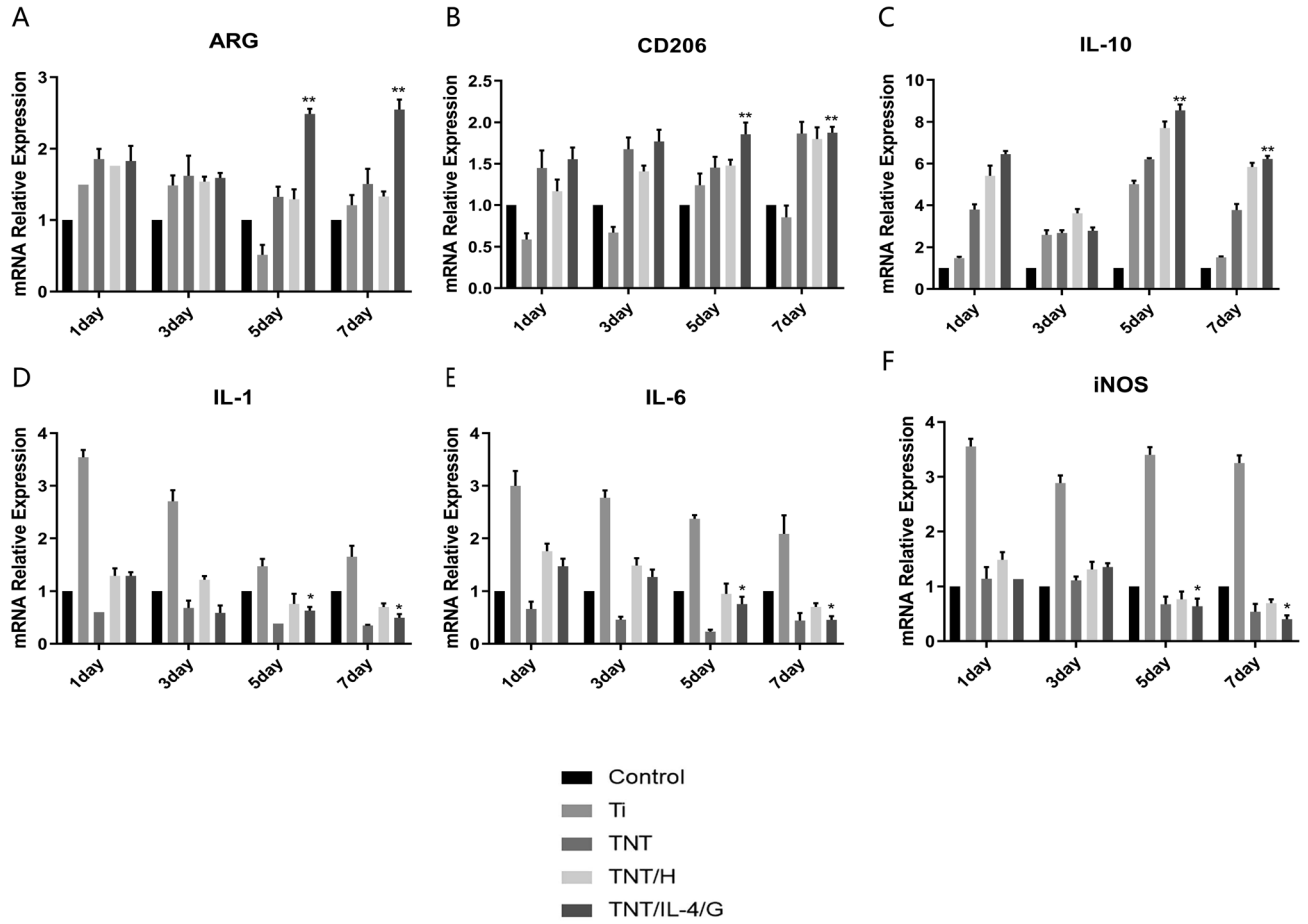

Fig. 4 Polarization analysis of macrophages. (A) The expression level of M2-related gene ARG was detected in macrophages after 1 d, 3 d, 5 d and 7 d culture. The method of (B)–(F) are the same as that of (A). Results are presented as mean, *$P < 0.05$, **$P < 0.01$.

TNT, TNT/H and TNT/IL-4/G were decreased compared with those in the Ti PBS liquid phase. The expression levels of the inflammatory factors in the TNT/IL-4/G decreased more significantly ($P < 0.01$). In contrast to these findings, the expression levels of IL-10 were mainly secreted by the M2-type macrophages that were significantly higher in the TNT/IL-4/G nanotubes compared with those of the control group (Fig. 5C) ($P < 0.05$). RT-PCR and ELISA data demonstrated that the expression levels of ARG, CD206 and IL-10, as well as the secretion of IL-10 inflammatory factors were significantly increased, while the expression levels of the IL-1, IL-6 and iNOS genes, as well as the secretion of IL-1, TNF-α and other inflammatory factors were significantly decreased. Therefore, it was reasonable to believe that the TNT/IL-4/G delivery system can promote M2-type polarization, and was more effective than TNT60 alone. This suggests that IL-4 exhibits its "promoter" effect.

Recent studies have identified various cytokines that can control the polarization of macrophages. It has also been recently shown that IL-33 and IL-21 are associated with M2 polarization.[17–19] IL-1 can inhibit macrophage activation, and is considered the "catalyst" of the M2 polarization.[20] IL-1 is mainly secreted by M1 cells, and can disrupt the tight connection of endothelial cells.[21] Excessive IL-8 release can also damage the growth of endothelial cells,[22] which may lead to the shedding of endothelial cells and the formation of platelet thrombosis. In contrast to IL-8, increased IL-10 secretion can effectively inhibit the production of pro-inflammatory cytokines.[23] Our data are consistent with most of the above points of view. Therefore, the polarization of macrophages can be controlled following implant introduction into the body. The fatal side effect of thrombus formation, following valve replacement, may be improved significantly.

Effect of CM-treated macrophages on the endothelialization of endothelial cells

The effect of macrophages grown in conditioned medium on endothelial cell behavior was comprehensively evaluated in terms of cell migration, tube formation, proliferation, and adhesion. As shown in Fig. 6A and D, the healing rate of all CM-treated cells at 12 h was higher than that of the control group, in which the healing rate of Ti-CM was approximately 23.68% ± 1.28%. The healing rate of TNT, TNT/H, and TNT/IL-4/G was approximately 47.50% ± 2.00%, 46.34% ± 1.38%, and 60.46% ± 2.34%, respectively, whereas the difference between the TNT/IL-4/G and TNT groups was significant ($P < 0.05$). In addition, with the exception of the control group, we observed the three-

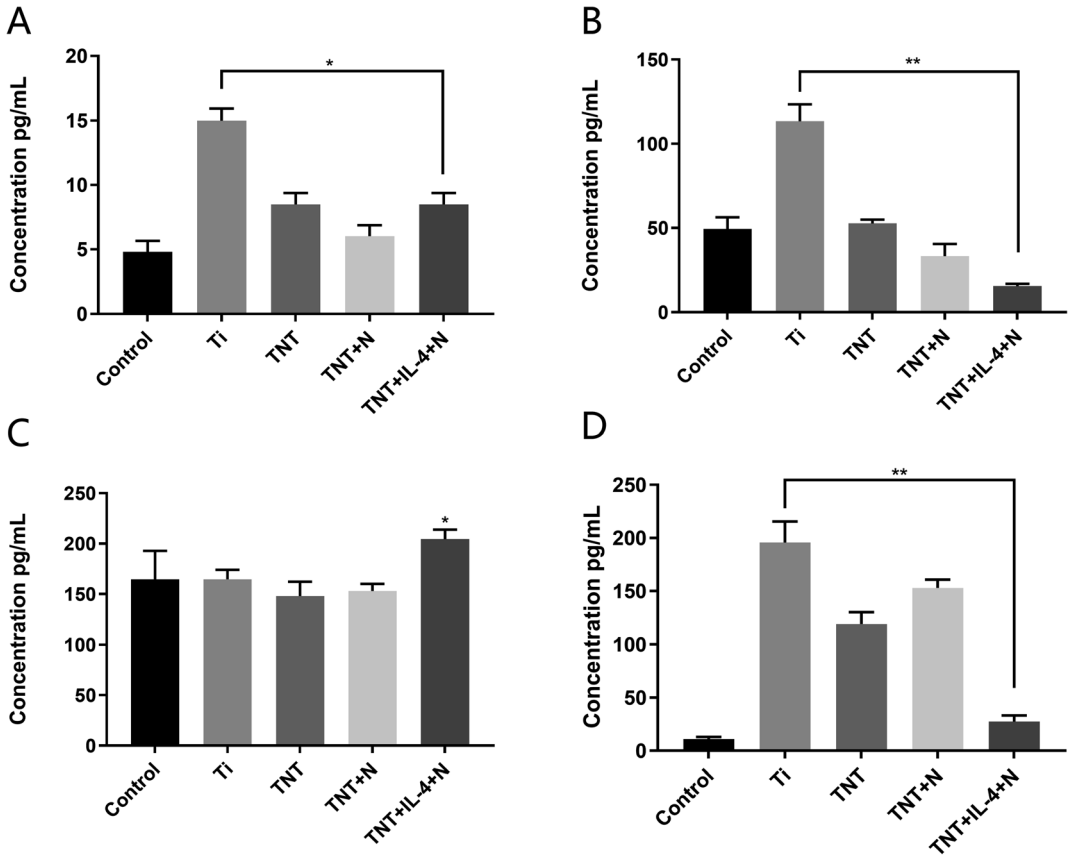

Fig. 5 The release of inflammatory cytokines. (A) The release of inflammatory factor IL-1 was detected in the superscript of different samples (Ti, TNT, TNT/H and TNT/IL-4/G). The method of (B)–(D) are same as (A). Results are presented as mean, *$P < 0.05$, **$P < 0.01$.

dimensional network structure in other groups. The network structure formed by the TNT/IL-4/G group was particularly dense (Fig. 6B). We conducted quantitative analysis on the number of new tube formation and header length of endothelial cells in all CM, and the data indicated that the parameters for new tube formation and header length exhibited the following order: TNT/IL-4/G > TNT > TNT/H > Ti. A significant difference was noted between TNT/IL-4/G and TNT ($P < 0.05$) (Fig. 6E and F). Concomitantly, CCK8 was used to determine cell proliferation. As shown in Fig. 6C, no proliferative differences were shown in each group at the three time points. The aforementioned data analysis suggested that both healing rate (reflecting cell migration) and tube formation of TNT/IL-4/G were better than those of other nanotubes (Ti, TNT and TNT/H). Each group promoted endothelialization to some extent. This effect was notably noted in the TNT/IL-4/G group.

Macrophages regulate angiogenesis by releasing a specific amount of cytokines at the right time, which is an extremely complex process.[24–27] We believe that it is some role of the inflammatory factors on endothelial cells in the conditioned medium of each group, which needs further study. Among them, VEGF is the most critical cytokine to promote angiogenesis.[28] In the late stage of tissue repair, M2 cells can secrete higher levels of VEGF, which can enhance the physiological activities of endothelial cells and eventually accelerate endothelialization, thus reducing the risk of thrombosis.[24,29] We collected the conditioned medium of TNT/IL-4/G co-cultured with macrophages, and used the conditioned medium of each group to cultivate endothelial cells, which greatly simulated the anti-inflammatory program in the body. Finally, the used TNT/IL-4/G changed the inflammatory response.

Anticoagulation efficiency

We confirmed that heparin would be gradually released from the hydrogel. In order to verify whether heparin could play an anticoagulant role after release, we tested BCT, aPTT/PT and platelet adhesion. The coagulation time of the blank control group did not exhibit a significant difference compared with that of the PBS (pH = 7.4), TNT and TNT/H groups (Fig. 7A). However, the coagulation time of the TNT/IL-4/G was significantly extended compared with that of the control group ($P < 0.05$). Similarly, the TNT/IL-4/G group exhibited a significantly longer coagulation time compared with that of the other two groups ($P < 0.01$). The three time points of 4, 8 and 12 h were selected to measure the values of aPTT and PT. The aPTT level of the blank group was basically the same as that of the TNT and TNT/H groups, while that of the TNT/IL-4/G group was considerably higher than that of the other three groups. The difference was highly significant at longer time periods of release ($P < 0.05$) (Fig. 7B). No significant difference was noted in the PT values

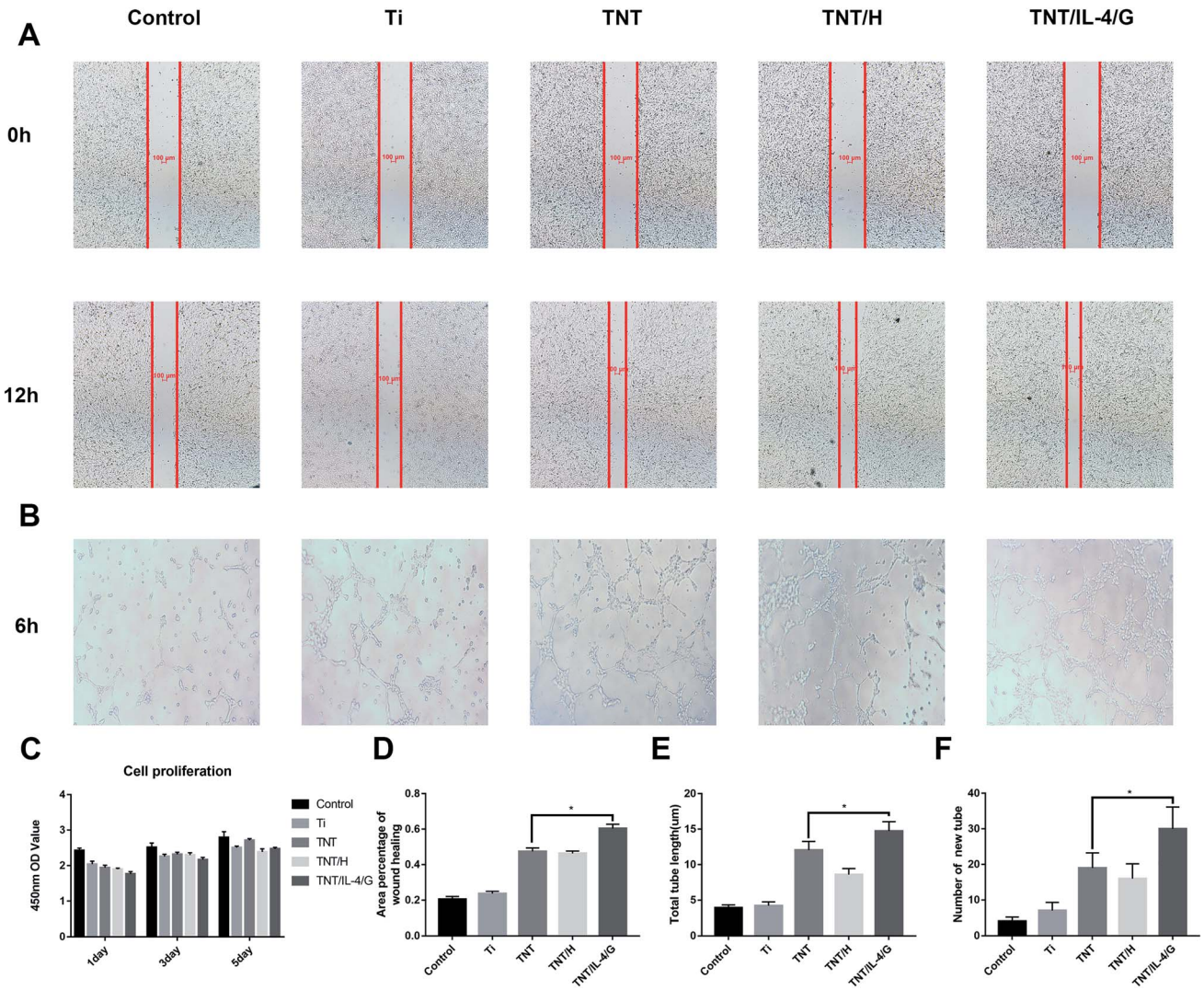

Fig. 6 Evaluation of the *in vitro* behaviors of HUVECs stimulated with conditioned medium. (A) Representative images of HUVEC migration. (B) Representative images of tube formation for 6 hours. (C) Cell proliferation in HUVECs for 1, 3, and 5 days. (D) The percentage of coverage after 6 hours of wound healing. (E) Quantitative analysis of the lengths of new tubes. (F) Quantitative analysis of the number of new tubes. Results are presented as mean, $*P < 0.05$, $**P < 0.01$.

among the four groups (Fig. 7C). Subsequently, we indirectly measured the concentration of platelets that adhered to the surface of the material using the LDH/LD kit for the different material groups. As shown in Fig. 7D, the concentration of platelet adhesion to the surface followed the following order: TNT/H > TNT > Ti > TNT/IL-4/G. The platelet levels in the TNT/IL-4/G group were significantly lower than those of the other three groups ($P < 0.05$). It could be intuitively noted that the platelet surface adhesion of the TNT/IL-4/G was indeed lower than that of the other three groups. After implantation of this delivery system *in vitro*, heparin is released and exerts its drug effect, which can be used for anticoagulant therapy after valve replacement.

Heparin is a very commonly used anticoagulant in clinical practice, and its anticoagulation effect has been well established.[30–32] Similarly, PT/aPTT is also a commonly used indicator of coagulation function in clinical practice. The chitosan/heparin has been shown to be effective in anticoagulation.[33–35] Our results also show that heparin in TNT/IL-4/G can be released stably and exert its anticoagulant effect. The chitosan covering the surface of the TNT can be combined with heparin to achieve sustained release. A study has also shown that loading heparin on hydrogels can reduce coagulation and enhance re-endothelialization of vascular lumen surfaces.[13]

In vivo angiogenesis

C57 female mice that underwent surgery were raised for 2 weeks and their back material was removed (Fig. 8A). H&E staining indicated that all materials were completely infiltrated by cells (Fig. 8B). In addition, we performed CD31 immunohistochemical staining. As shown in Fig. 8C, with the exception of Ti, macrovascular structures appeared in all treatment groups

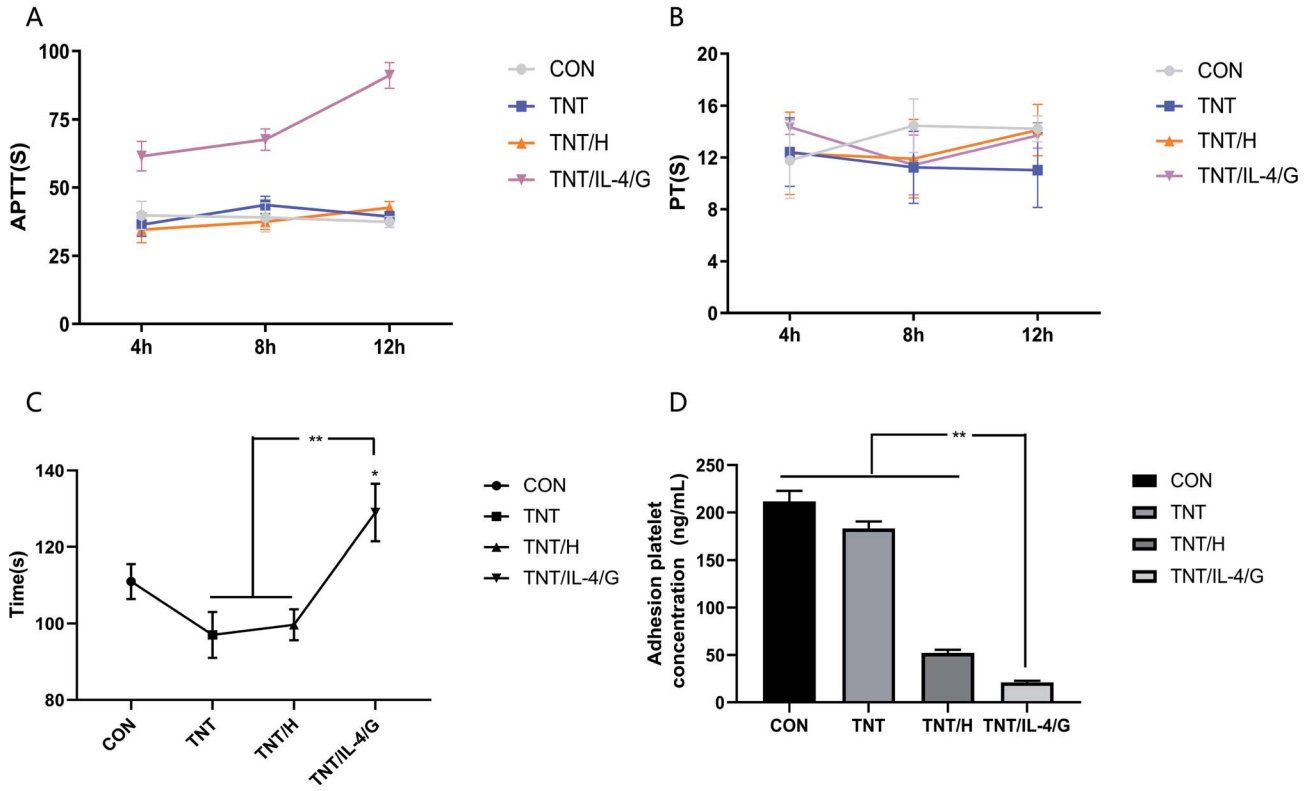

Fig. 7 Anticoagulation and antiplatelet experiments of nanomaterials. (A) aPTT values of different samples (con, TNT, THT/H and TNT/IL-4/G) were detected at 4 h, 8 h and 12 h, respectively. (B) PT values of different samples (con, TNT, THT/H and TNT/IL-4/G) were detected at 4 h, 8 h and 12 h, respectively. (C) The coagulation time of different samples was measured after 12 hours of incubation at 37 °C. (D) Adhesive platelet concentrations of Ti, TNT, TNT/H and TNT/IL-4/G were indirectly detected by kit after incubation at 37 °C for 12h. Results are presented as mean, $*P < 0.05$, $**P < 0.01$.

(TNT, TNT/H and TNT/IL-4/G), and the macrovascular structures in the TNT/IL-4/G group were significantly higher than those noted in the TNT and TNT/H groups. A significantly higher number of $CD31^+$ blood vessels was noted in the TNT/IL-4/G group compared with that of the TNT group ($P < 0.05$) (Fig. 8D).

Judging from all of the experimental data, whether *in vitro* or *in vivo*, TNT/IL-4/G showed good endothelialization ability, which verified our initial hypothesis. It follows that application of titanium-based biomaterials to regulate the behavior of blood and endothelial cells by changing their surface properties, thus improving the performance and function of materials or devices, has important scientific and practical significance.

To date, the studies that have examined the association of IL-4 with TNT and the phenotypic transformation of macrophages have attracted considerable attention.[36,37] Yin *et al.* reported the release of IL-4 on TNT. A cross-linked PEM membrane was formed on the surface to regulate the phenotype of macrophages *via* the sustained release of IL-4.[38] In addition, a hydrogel layer/heparin was applied to the scaffold surface to rapidly release heparin using hydrogel hydrophilicity and to reduce stent thrombosis.[39] In addition, the TNT/IL-4/IFN-γ delivery system was designed by IL-4 and hydrogel, and the phenotype transformation of the macrophages was regulated.[40] These studies designed new delivery systems using IL-4-loaded TNT. In addition to the above studies, many other studies have discussed the key role of titanium implants in anti-inflammatory responses, and highlighted the important role of nanostructured surfaces.[41–45] However, most of these studies have focused on the proliferation, adhesion, and secretion of proinflammatory cytokines on macrophages.[44] Problems with accurate *in situ* administration, poor local retention, and the high cost of producing the necessary amounts of growth factors currently limit these methods.[46] It may be more promising to use their own cells to solve these problems, and macrophages are the "secretors".

To sum up, this study constructed a TNT/IL-4/G drug delivery system to accelerate endothelialization and anticoagulation, and designed an experiment to greatly simulate the effect of macrophages on endothelial cells in the anti-inflammatory process of the body, and used the TNT/IL-4/G drug delivery system to intervene and make macrophages transform to an anti-inflammatory phenotype. M2 type macrophages secrete more VEGF, which accelerates endothelialization. At the same time, heparin continues to release from the hydrogel and finally achieves anticoagulation. However, we need additional experiments to study the specific mechanism. For example, the mediation mechanism of VEGF on endothelial cells. Therefore, TNT/IL-4/G delivery system can be used as a functional carrier for antithrombotic and anticoagulant. Based on its performance, the artificial valve materials are expected to be improved and even replaced in the future.

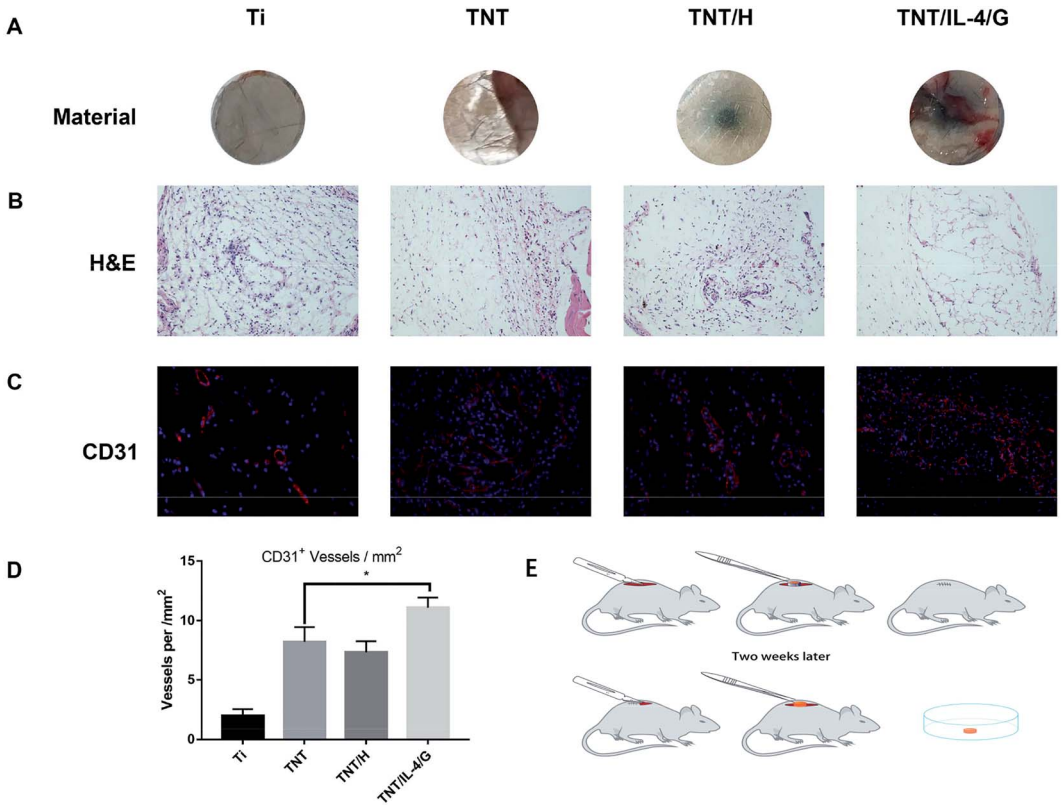

Fig. 8 *In vivo* angiogenesis. (A) Subcutaneous implantation of materials (Ti, TNT, TNT/H and TNT/IL-4/G) in mice after 2 weeks. (B) H&E staining. (C) Immunohistochemical analysis of endothelial cell markers CD31 and DAPI. (D) Quantification of the number of $CD31^+$ vessels per mm^2. (E) Schematic diagram of *in vivo* angiogenesis experiment; all the mice used were of the same strain, age and gender. Results are presented as mean, $^*P < 0.05$, $^{**}P < 0.01$.

Conclusion

The results indicated that biofunctionalization of the titanium nanotube with the chitosan/genipin heparin hydrogel and the controlled release of IL-4 had a significant regulatory effect on macrophage polarization. Macrophages on the surface of TNT in each group were M2-polarized. Among these, the TNT/IL-4/G group exhibited the most significant effect. The expression levels of the M2-type-related genes were upregulated and the secretion of inflammatory factors was decreased. In addition, the conditioned medium of the macrophages could promote a series of physiological behaviors of endothelial cells, and accelerate the process of endothelialization. Heparin release by the TNT/IL-4/G indicated a significant anticoagulation effect *in vitro*. Therefore, we believe that biofunctionalization of the titanium nanotube with the chitosan/genipin heparin hydrogel and the controlled release of IL-4 can achieve rapid endothelialization and anticoagulation.

Author contributions

Wen Peng Yu and Yi Gong carried out the experiments. Chao Lu and Xin Liang Liu prepared the manuscript. Jian Liang Zhou and Jing Li Ding designed the experiments. Jian Jun Xu and Ziyao Wang analyzed the experimental results. Feng Lin and Guo Dong Zhu revised the manuscript. All authors reviewed the manuscript. All authors contributed to the data analysis, drafting or revising the article, gave final approval of the version to be published, and agree to be accountable for all aspects of the work.

Statement

All animal procedures were performed in accordance with the Guidelines for Care and Use of Laboratory Animals of Nanchang University, and approved by the Animal Ethics Committee of Nanchang University.

Conflicts of interest

There are no conflicts to declare.

Acknowledgements

This work was funded by the National High-tech Research and Development Program (863 Program) of China (grant no. 2014AA020539), the National Natural Science Foundation of China (grant no. 81770388, 81860079, and 81660070), the Natural Science Foundation of Jiangxi Province (grant no. 20171ACB21061 and 20192BAB205070), and the Research

Project of Jiangxi Provincial Department of Education (grant no. 150274).

References

1 A. de Mel, G. Jell, M. M. Stevens and A. M. Seifalian, Biofunctionalization of biomaterials for accelerated *in situ* endothelialization: a review, *Biomacromolecules*, 2008, **9**(11), 2969–2979.

2 K. Kalantari, B. Saleh and T. J. Webster, Biological Applications of Severely Plastically Deformed Nano-Grained Medical Devices: A Review, *Nanomaterials*, 2021, **11**, 748.

3 D. Khudhair, A. Bhatti, Y. Li, *et al.*, Anodization parameters influencing the morphology and electrical properties of TiO2 nanotubes for living cell interfacing and investigations, *Mater. Sci. Eng., C*, 2016, **59**, 1125–1142.

4 J. Li, W. Qin, K. Zhang, *et al.*, Controlling mesenchymal stem cells differentiate into contractile smooth muscle cells on a TiO2 micro/nano interface: Towards benign pericytes environment for endothelialization, *Colloids Surf., B*, 2016, **145**, 410–419.

5 M. R. Major, V. W. Wong, E. R. Nelson, M. T. Longaker and G. C. Gurtner, The foreign body response: at the interface of surgery and bioengineering, *Plast. Reconstr. Surg.*, 2015, **135**(5), 1489–1498.

6 S. Franz, S. Rammelt, D. Scharnweber and J. C. Simon, Immune responses to implants - a review of the implications for the design of immunomodulatory biomaterials, *Biomaterials*, 2011, **32**(28), 6692–6709.

7 A. Mantovani, A. Sica, S. Sozzani, P. Allavena, A. Vecchi and M. Locati, The chemokine system in diverse forms of macrophage activation and polarization, *Trends Immunol.*, 2004, **25**(12), 677–686.

8 C. Chu, L. Liu, S. Rung, *et al.*, Modulation of foreign body reaction and macrophage phenotypes concerning microenvironment, *J. Biomed. Mater. Res., Part A*, 2020, **108**(1), 127–135.

9 Q. Lin, X. Ding, F. Qiu, X. Song, G. Fu and J. Ji, *In situ* endothelialization of intravascular stents coated with an anti-CD34 antibody functionalized heparin-collagen multilayer, *Biomaterials*, 2010, **31**(14), 4017–4025.

10 S. Patel-Hett and P. A. D'Amore, Signal transduction in vasculogenesis and developmental angiogenesis, *Int. J. Dev. Biol.*, 2011, **55**(4–5), 353–363.

11 Z. Gong, Y. Hu, F. Gao, *et al.*, Effects of diameters and crystals of titanium dioxide nanotube arrays on blood compatibility and endothelial cell behaviors, *Colloids Surf., B*, 2019, **184**, 110521.

12 M. E. A. El-Hack, M. T. El-Saadony, M. E. Shafi, *et al.*, Antimicrobial and antioxidant properties of chitosan and its derivatives and their applications: A review, *Int. J. Biol. Macromol.*, 2020, **164**, 2726–2744.

13 T. Groth and A. Lendlein, Layer-by-layer deposition of polyelectrolytes – a versatile tool for the *in vivo* repair of blood vessels, *Angew. Chem., Int. Ed. Engl.*, 2004, **43**(8), 926–928.

14 M. Kim and C. Cha, Integrative control of mechanical and degradation properties of *in situ* crosslinkable polyamine-based hydrogels for dual-mode drug release kinetics, *Polymer*, 2018, **145**, 272–280.

15 K. Lee, J. Hong, H. J. Roh, *et al.*, Dual ionic crosslinked interpenetrating network of alginate-cellulose beads with enhanced mechanical properties for biocompatible encapsulation, *Cellulose*, 2017, **24**(11), 4963–4979.

16 S. K. Biswas and A. Mantovani, Macrophage plasticity and interaction with lymphocyte subsets: cancer as a paradigm, *Nat. Immunol.*, 2010, **11**(10), 889–896.

17 L. D. Hazlett, S. A. McClellan, R. P. Barrett, *et al.*, IL-33 shifts macrophage polarization, promoting resistance against Pseudomonas aeruginosa keratitis, *Invest. Ophthalmol. Visual Sci.*, 2010, **51**(3), 1524–1532.

18 M. Kurowska-Stolarska, B. Stolarski, P. Kewin, *et al.*, IL-33 amplifies the polarization of alternatively activated macrophages that contribute to airway inflammation, *J. Immunol.*, 2009, **183**(10), 6469–6477.

19 J. Pesce, M. Kaviratne, T. R. Ramalingam, *et al.*, The IL-21 receptor augments Th2 effector function and alternative macrophage activation, *J. Clin. Invest.*, 2006, **116**(7), 2044–2055.

20 S. Gordon, Alternative activation of macrophages, *Nat. Rev. Immunol.*, 2003, **3**(1), 23–35.

21 G. Tossetta, F. Paolinelli, C. Avellini, *et al.*, IL-1β and TGF-β weaken the placental barrier through destruction of tight junctions: an *in vivo* and *in vitro* study, *Placenta*, 2014, **35**(7), 509–516.

22 Y. Amir Levy, T. P. Ciaraldi, S. R. Mudaliar, S. A. Phillips and R. R. Henry, Excessive secretion of IL-8 by skeletal muscle in type 2 diabetes impairs tube growth: potential role of PI3K and the Tie2 receptor, *Am. J. Physiol.: Endocrinol. Metab.*, 2015, **309**(1), E22–E34.

23 B. T. Ameredes, R. Zamora, K. F. Gibson, *et al.*, Increased nitric oxide production by airway cells of sensitized and challenged IL-10 knockout mice, *J. Leukocyte Biol.*, 2001, **70**(5), 730–736.

24 K. L. Spiller, R. R. Anfang, K. J. Spiller, *et al.*, The role of macrophage phenotype in vascularization of tissue engineering scaffolds, *Biomaterials*, 2014, **35**(15), 4477–4488.

25 M. Anghelina, P. Krishnan, L. Moldovan and N. I. Moldovan, Monocytes and macrophages form branched cell columns in matrigel: implications for a role in neovascularization, *Stem Cells Dev.*, 2004, **13**(6), 665–676.

26 N. Hibino, T. Yi, D. R. Duncan, *et al.*, A critical role for macrophages in neovessel formation and the development of stenosis in tissue-engineered vascular grafts, *FASEB J.*, 2011, **25**(12), 4253–4263.

27 P. J. Murray and T. A. Wynn, Protective and pathogenic functions of macrophage subsets, *Nat. Rev. Immunol.*, 2011, **11**(11), 723–737.

28 R. J. Galas Jr and J. C. Liu, Surface density of vascular endothelial growth factor modulates endothelial proliferation and differentiation, *J. Cell. Biochem.*, 2014, **115**(1), 111–120.

29 K. L. Spiller, S. Nassiri, C. E. Witherel, *et al.*, Sequential delivery of immunomodulatory cytokines to facilitate the M1-to-M2 transition of macrophages and enhance vascularization of bone scaffolds, *Biomaterials*, 2015, **37**, 194–207.

30 P. W. Serruys, B. van Hout, H. Bonnier, *et al.*, Randomised comparison of implantation of heparin-coated stents with balloon angioplasty in selected patients with coronary artery disease (Benestent II), *Lancet*, 1998, **352**(9129), 673–681.

31 P. W. Serruys, H. Emanuelsson, W. van der Giessen, *et al.*, Heparin-coated Palmaz-Schatz stents in human coronary arteries. Early outcome of the Benestent-II Pilot Study, *Circulation*, 1996, **93**(3), 412–422.

32 P. A. Hårdhammar, H. M. van Beusekom, H. U. Emanuelsson, *et al.*, Reduction in thrombotic events with heparin-coated Palmaz-Schatz stents in normal porcine coronary arteries, *Circulation*, 1996, **93**(3), 423–430.

33 J. Fu, J. Ji, W. Yuan and J. Shen, Construction of anti-adhesive and antibacterial multilayer films *via* layer-by-layer assembly of heparin and chitosan, *Biomaterials*, 2005, **26**(33), 6684–6692.

34 J. Fu, J. Ji, D. Fan and J. Shen, Construction of antibacterial multilayer films containing nanosilver *via* layer-by-layer assembly of heparin and chitosan-silver ions complex, *J. Biomed. Mater. Res., Part A*, 2006, **79**(3), 665–674.

35 T. Serizawa, M. Yamaguchi and M. Akashi, Alternating bioactivity of polymeric layer-by-layer assemblies: anticoagulation *vs.* procoagulation of human blood, *Biomacromolecules*, 2002, **3**(4), 724–731.

36 L. Gao, M. Li, L. Yin, *et al.*, Dual-inflammatory cytokines on TiO2 nanotube-coated surfaces used for regulating macrophage polarization in bone implants, *J. Biomed. Mater. Res., Part A*, 2018, **106**(7), 1878–1886.

37 M. Li, L. Gao, J. Chen, *et al.*, Controllable release of interleukin-4 in double-layer sol-gel coatings on TiO2 nanotubes for modulating macrophage polarization, *Biomed. Mater.*, 2018, **13**(4), 045008.

38 X. Yin, Y. Li, C. Yang, *et al.*, Alginate/chitosan multilayer films coated on IL-4-loaded TiO2 nanotubes for modulation of macrophage phenotype, *Int. J. Biol. Macromol.*, 2019, **133**, 503–513.

39 S. Meng, Z. Liu, L. Shen, *et al.*, The effect of a layer-by-layer chitosan-heparin coating on the endothelialization and coagulation properties of a coronary stent system, *Biomaterials*, 2009, **30**(12), 2276–2283.

40 J. Chen, M. Li, C. Yang, *et al.*, Macrophage phenotype switch by sequential action of immunomodulatory cytokines from hydrogel layers on titania nanotubes, *Colloids Surf., B*, 2018, **163**, 336–345.

41 *Encyclopedia of Biomedical Engineering*, ed. N. P. Rhodes, Elsevier, 2019, pp. 242–248.

42 J. W. Park, S. H. Han and T. Hanawa, Effects of Surface Nanotopography and Calcium Chemistry of Titanium Bone Implants on Early Blood Platelet and Macrophage Cell Function, *BioMed Res. Int.*, 2018, **2018**, 1362958.

43 Q. L. Ma, L. Z. Zhao, R. R. Liu, *et al.*, Improved implant osseointegration of a nanostructured titanium surface *via* mediation of macrophage polarization, *Biomaterials*, 2014, **35**(37), 9853–9867.

44 W. L. Lü, N. Wang, P. Gao, C. Y. Li, H. S. Zhao and Z. T. Zhang, Effects of anodic titanium dioxide nanotubes of different diameters on macrophage secretion and expression of cytokines and chemokines, *Cell Proliferation*, 2015, **48**(1), 95–104.

45 J. Wang, F. Meng, W. Song, *et al.*, Nanostructured titanium regulates osseointegration *via* influencing macrophage polarization in the osteogenic environment, *Int. J. Nanomed.*, 2018, **13**, 4029–4043.

46 M. L. Iruela-Arispe, A dual origin for blood vessels, *Nature*, 2018, **562**(7726), 195–197.